

# Isolation and Sequencing of *Actin1*, *Actin2* and *Tubulin1* Genes Involved in Cytoskeleton Formation in *Phytophthora cinnamomi*

Ivone M Martins<sup>1,2</sup>, M Carmen López<sup>3</sup>, Angél Dominguez<sup>3</sup> and Altino Choupina<sup>1,2\*</sup>

<sup>1</sup>Department of Biology and Biotechnology, Polytechnic Institute of Bragança, Apartado 1172, 5301-854 Bragança, Portugal

<sup>2</sup>Mountain Research Center, Polytechnic Institute of Bragança, Apartado 1172, 5301-854 Bragança, Portugal

<sup>3</sup>Department of Microbiology and Genetics, CIETUS-IBSAL, University of Salamanca / CSIC, Plaza de Drs. Queen s/n, 37007 Salamanca, Spain

## Abstract

Oomycetes from the genus *Phytophthora* are fungus-like plant pathogens that are devastating for agriculture and natural ecosystems. On the Nordeste Transmontano region (northeast Portugal), the *Castanea sativa* chestnut culture is extremely important. The biggest productivity and yield break occurs due to the ink disease, caused by *Phytophthora cinnamomi* which is one of the most widely distributed *Phytophthora* species, with nearly 1000 host species. The knowledge about molecular mechanisms responsible for pathogenicity is an important tool in order to combat associate diseases of this pathogen. Complete open reading frames (ORFs) of *act1*, *act2* and *tub1* genes who participate in cytoskeleton formation in *P. cinnamomi* were achieved by high-efficiency thermal asymmetric interlaced (HE-TAIL) polymerase chain reaction (PCR). *act1* gene comprises a 1128 bp ORF, encoding a deduced protein of 375 amino acids (aa) and 41,972 kDa. *act2* ORF comprises 1083 bp and encodes a deduced protein of 360 aa and 40,237 kDa. *tub1* has a total length of 2263 bp and encodes a 453 aa protein with a molecular weight of 49.911 kDa. Bioinformatics analyses shows that *actin1* is ortholog to the *act1* genes of *Phytophthora infestans*, *Phytophthora megasperma* and *Phytophthora melonis*; *actin2* is ortholog to the *act2* genes of *P. infestans*, *Phytophthora brassicae*, *P. melonis* and *Pythium splendens* and *tubulin1* shows the highest orthology to *P. infestans* and *P. capsici*  $\alpha$ -tubulin genes.

Analysed 3D structure of the three putative proteins revealed a spatial conformation highly similar to those described for orthologous proteins obtained by X-ray diffraction.

**Keywords:** Actin; *Castanea sativa*; Cytoskeleton; Ink disease; *Phytophthora cinnamomi*; Tubulin

## Introduction

*Phytophthora cinnamomi* is a destructive and widespread soil-borne oomycete that infects woody plant hosts [1]. On the Nordeste Transmontano region (northeast Portugal), this pathogen is the responsible by the ink disease affecting *Castanea sativa* chestnut. The most common symptoms are root necrosis and reduction in root growth, which invariably lead to tree death [2]. Due to their particular physiological characteristics, no efficient treatments against diseases caused by these microorganisms are presently available [3]. In order to develop such treatments appeared essential to dissect the molecular mechanisms of the interaction between *Phytophthora* species and host plants.

Actin and tubulin are highly abundant conserved proteins in eukaryotic cells, which participate in more protein-protein interactions than any other proteins [4,5]. These properties, together with the actin capacity to carry out the transition between monomeric (G-actin) and filamentous (F-actin) states under the control of nucleotide hydrolysis, ions, and a large number of actin-binding proteins, make actin a critical player in many cellular functions, ranging from cell motility and the maintenance of cell shape and polarity to the regulation of transcription [6,7]. In vertebrates there are three groups of actin isoforms: alpha, beta and gamma. The alpha actins are found in muscle tissues and are a major constituent of the contractile apparatus. The beta and gamma actins co-exist in most cell types as components of the cytoskeleton and act as mediators of internal cell motility. In plants there are many isoforms which are probably involved in a variety of functions such as cytoplasmic streaming, cell shape determination, tip growth, graviperception, cell wall deposition, etc.

A moderate-sized protein consisting of approximately 375 residues, actin is encoded by a large, highly conserved, gene family. Some single-celled eukaryotes like yeasts and amoebae have a single actin gene, whereas many multicellular organisms contain multiple actin genes. Actin in *Phytophthora infestans* is encoded by at least two genes, *actA* and *actB*, in contrast to unicellular and filamentous fungi *Saccharomyces cerevisiae*, *Kluyveromyces lactis* and *Yarrowia lipolytica*, where a single gene have been detected [8,9]. On the other hand microtubules are major constituents of the cell cytoskeleton participating in a wide range of cellular functions, such as motility, division, maintenance of cell shape, and intracellular transport. Also play an essential role in nuclear division as components of the mitotic spindle and dimeric tubulin is their primary component. A key property of tubulin is its ability to assemble into microtubules via interaction between polymerized  $\alpha$ - and  $\beta$ -tubulin monomers (heterodimer), and to undergo disassembly at appropriate times in the cell cycle. However, microtubule role is variable depending on the organism, cell type and other factors.

**\*Corresponding author:** Altino Choupina, Department of Biology and Biotechnology, Polytechnic Institute of Bragança, Apartado 1172, 5301-854 Bragança, Portugal, Tel: +351 273303371; Fax: +351 273325405; E-mail: [albracho@ipb.pt](mailto:albracho@ipb.pt)

Received July 19, 2013; Accepted August 21, 2013; Published August 28, 2013

**Citation:** Martins IM, López MC, Dominguez A, Choupina A (2013) Isolation and Sequencing of *Actin1*, *Actin2* and *Tubulin1* Genes Involved in Cytoskeleton Formation in *Phytophthora cinnamomi*. J Plant Pathol Microb 4: 194 doi:[10.4172/2157-7471.1000194](https://doi.org/10.4172/2157-7471.1000194)

**Copyright:** © 2013 Martins IM, et al. This is an open-access article distributed under the terms of the Creative Commons Attribution License, which permits unrestricted use, distribution, and reproduction in any medium, provided the original author and source are credited.

The aim of this study was to isolate and sequence three genes involved in cytoskeleton formation in *P. cinnamomi*.

## Materials and Methods

### Biological material

*P. cinnamomi* isolate Pr120 was isolated from soil samples from sites of *C. sativa* affected by the ink disease on the Nordeste Transmontano region (northeast Portugal). The strain was grown in the dark for 4-6 days at 22-25°C in PDA (Potato-Dextrose Agar) medium. This isolate is preserved at the Laboratory of Molecular Biology of the Polytechnic Institute of Bragança (IPB).

Total genomic DNA from *P. cinnamomi* mycelium was isolated according to the reported methods [10,11].

### Fluorescence microscopy

For nuclei staining, *P. cinnamomi* mycelium was grown in PDA medium and resuspended in PBS 10X containing 1 mg/ml of Dapi (4-6-Diamidino-2-phenylindole) (Sigma-Aldrich), and visualized with the appropriate UV filter. For cell wall staining, *P. cinnamomi* mycelium was grown in PDA medium and resuspended in PBS 10X containing 10 mg/ml of Calcofluor white (Sigma-Aldrich), using the appropriate UV filter. For actin visualization, *P. cinnamomi* mycelium was grown in PDA medium and stained with 0.1 µg/ml rhodamine-conjugated phalloidin (Invitrogen) [12]. Images were obtained using a Leica HC (Germany) fluorescence microscope, type 020-523.010.

### Amplification of the actin and tubulin genes

PCR was used to amplify *act1*, *act2* and *tub1* genes from *P. cinnamomi*. Degenerated primers Act1 (5'-GYMATGGASGAC-GAYATTCARGC-3') and Act2 (5'-GYMGYCTTAGAAGCACTT-GCGRTG) to amplify *act1*, Act3 (5'-CAWTC AAGATGGCTGAC-GAWGAYG) and Act4 (5'-CARCTTAGAAGCACT TGCGGTGC) to amplify *act2*, were designed based on actin A and B sequences alignment from *P. infestans*. Degenerated primers Tub1 (5'-GGYAATGC-STGTTGGGAAYTMTAT) and Tub2 (5'-CATMCCYTCWCCSAC RTACCAGTG) to amplify *tub1*, were designed based on α-tubulin sequences alignment from *S. cerevisiae* and *P. palmivora*. The thermal program used for PCR reactions consisted of one cycle of 94°C for 5 min, 30 cycles of 94°C for 30 sec; 57°C for 30 sec; 72°C for 1.5 min and 1 cycle of 72°C for 7 min. Each 25 µl PCR contained 0.8 mM dNTPs, 0.2 mM of each primer, 100 ng genomic DNA, and 2.5 U Taq DNA polymerase in the appropriate buffer. Aliquots of the PCR reactions were separated on 0.8% w/v agarose gels and stained with ethidium bromide, to check for the presence of the expected amplicon. PCR fragments were purified with "DNA and Gel Band Purification" kit (GE Healthcare), following the manufacturer's instructions. Amplified DNA was cloned into pGEM-T Easy (Promega) which is a linearized high-copy-number vector with a single 3'-terminal thymidine at both ends.

### Bacterial transformation and DNA extraction

Plasmids were propagated in *Escherichia coli* (DH5α cells, [13]) and plasmid DNA was extracted-purified with the Wizard® Plus SV Minipreps DNA Purification System (Promega), following the manufacturer's instructions. Both DNA fragments obtained were sequenced in a capillar automatic sequencer 3100 Genetic Analyzer (Applied Biosystem).

### Amplify unknown genomic DNA sequence of *act1*, *act2* and *tub1* genes

HE-TAIL PCR is an efficient method to amplify unknown genomic DNA sequences adjacent to short known regions by flanking the known sequence with asymmetric PCR. In this procedure gene specific primers, Act1.1 (5'-GCCGTTYTCCTTGATCAGCGG), Act1.2 (5'-AGGCGTTGTCGCCCCAGACC), Act2.1 (5'-CGGCCGCGGT-GACGCTGACG) and Act2.2 (5'-GGTCTGGGGCGACAACGCCT) were used to amplify unknown genomic DNA sequences of *act1* and *act2* genes. Gene specific primers Tub1.1 (5'-GCGTTGAACACCAG-GAAACCCTG) and Tub1.2 (5'-CGAGATCACCAACAGCGCCTTC-GA) were used to amplify unknown genomic DNA sequence of *tub1* gene. Degenerated primers R1 (5'-NGTCGASWGANAWGAA), R2 (5'-GTNCGASWCANAWGTT), R3 (5'-WGTGNAGWANCANA-GA) and R4 (5'-NCAGCT WSCNTSCTT) were applied [14]. Three rounds of PCR were performed using the product of the previous PCR as a template for the next (Table 1).

The primary PCR was performed in a 50 µl volume containing 80 ng of genomic DNA, 0.2 mM of primers M1 or M3 2 mM of a random primer (R1, R2, R3, R4), 0.2 mM of each dNTP and 1U Taq DNA polymerase in the appropriate buffer. The secondary PCR was performed with primers M2 or S4 (0.2 mM) and the same random primer R (2 mM) as used in the primary reaction. 1 µl of 1/50 dilution of the primary PCR was used as a template. Single-step annealing-extension PCR consisting of a combined annealing and extension step at 65°C or 68°C was used in primary and secondary PCR reactions. The tertiary reaction was carried out with 1 µl of 1/10 dilution of the secondary reaction, 0.2 mM of primers S1 and S2, 0.2 mM of random primer R (the same as used in the previous cycles), 0.2 mM of each dNTP, 1U DNA Taq polymerase in the appropriate buffer. To exclude nonspecific amplification, a tertiary control reaction R-R was set up without adding gene-specific primers.

### Amplification of promoter and terminator sequences of *act1*, *act2* and *tub1* genes

In this procedure gene-specific primers were designed and, in combination with those, the degenerated primer R2 was applied [14]. Three rounds of PCR were performed using the product of the previous PCR as a template for the next. A detailed cycler program is given in Table 1.

Reaction	Number of cycles	Thermal settings
Primary	1	93°C (1 min); 95°C (5 min)
	5	94°C (30 sec); 62°C (1 min); 72°C (2 min 30 sec)
	1	94°C (30 sec); 25°C ramping 72°C (3 min); 72°C (2 min 30 sec)
	15	94°C (20 sec); 65°C (3 min 30 sec); 94°C (20 sec); 65°C (3 min 30 sec); 94°C (30 sec); 42°C (1min); 72°C (2 min 30 sec)
	1	72°C (5 min); 4°C Hold
Secondary	12	94°C (20 sec); 65°C (3 min 30 sec); 94°C (20 sec); 65°C (3 min 30 sec); 94°C (30 sec); 42°C (1 min); 72°C (2 min 30 sec)
	1	72°C (5 min); 4°C Hold
	Tertiary	30
	1	72°C (5 min); 4°C Hold

**Table 1: HE-TAIL PCR cycle settings.** Primary, secondary and tertiary nested PCR reactions were performed sequentially. The primary PCR reaction consists of 15 TAIL cycles, while the secondary reaction contains 12 TAIL cycles.

The primary PCR was performed in a 50 µl volume containing 80 ng of genomic DNA, 0.1 mM of gene-specific primers, 2 mM of primer R2, 0.2 mM of each dNTP and 1U Taq DNA polymerase in the appropriate buffer. The secondary PCR was performed with gene-specific primers (0.2 mM) and the same primer R (2 mM) as used in the primary reaction. 1 µl of 1/50 dilution of the primary PCR was used as a template. Single-step annealing-extension PCR consisting of a combined annealing and extension step at 65°C or 68°C was used in primary and secondary PCR reactions. The tertiary reaction was carried out with 1 µl of 1/10 dilution of the secondary reaction, 0.2 mM of gene-specific primers, 0.2 mM of primer R2, 0.2 mM of each dNTP, 1U DNA Taq polymerase in the appropriate buffer. To exclude nonspecific amplification, a tertiary control reaction R2-R2 was set up without adding gene-specific primers.

### Protein structure analysis

The 3D structure of the proteins was achieved by using the PyMOL 1.3 r1 edu program and Swiss Model [15-17].

## Results and Discussion

### Microscopy visualization

In order to visualize the morphology of *P. cinnamomi* a staining and microscopic observation of three cell structures was performed (Figure 1): nucleus, through DAPI staining (Figure 1A). Each mycelium presents more than one individualized nucleus. Cell wall was observed by staining with calcofluor white (Figure 1B) who indicated the lack of division septa and actin cytoskeleton and according to [1]. Actin cytoskeleton was visualized with rhodamin-phalloidin, although actin distribution can be observed throughout all the mycelium, appeared more concentrated at the hyphae extremities and adjacent to the plasma membrane (Figure 1C), according to [7]. In oomycetes actin forms a cap immediately after the apical plasma membrane, whereas in other organisms like *P. cinnamomi*, the actin appears in small plates in the tips of hyphae [7].

Hypha of *P. cinnamomi* also shows strong punctate staining in the sub-apical region, and strong staining bands along the walls of the hypha. Some evidences suggest that microfilaments reinforce the hypha tip of oomycetes. Disruption of the F-actin cap and reduction of F-actin at the tips of oomycetes hypha could, along with cell wall softening, increase tip yielding and thus playing a potential role in invasive hypha growth [7].

### *act1*, *act2* and *tub1* amplification

Performing a PCR using genomic DNA from *P. cinnamomi* as template and degenerated primers designed based on actin A and B sequences alignment from *P. infestans*, and the  $\alpha$ -tubulin sequences alignment from *S. cerevisiae* and *P. palmivora*, we were able to amplify three fragments of about 1200 bp.

After sequencing and bioinformatics analysis, we found that our sequences presented identity with several sequences of the database with the characteristic actin and tubulin domains. We named our sequences Actin1, Actin2 and Tubulin1, EMBL database, accession numbers AM412175.1, AM412176.1 and AM412177.1, respectively.

After performing a HE-TAIL PCR, the fragments of interest were selected and sequenced. By using BioAlign and SeqMan programs we were able to align and analyse the sequences. Through this method we could amplify both promoter (+113 bp) and terminator (+640 bp) of the *act1* gene. We were not able to amplify the promoter and terminator of the *act2* gene because the sequences that we isolated and should flank this gene did not align with the original fragment. For the *tub1* gene we could amplify both promoter (+352 bp) and terminator (+549 bp) regions.

A BLAST analysis (blast.ncbi.nlm.nih.gov) of both genes was performed against *Phytophthora*, *Saccharomyces cerevisiae*, *Kluyveromyces lactis* and *Aspergillus nidulans*. *act1* and *act2* of *P. cinnamomi* present an identity of 88%. *act1* present an identity of 100% against *P. infestans*, *P. megasperma* and *P. melonis* and *act2* is ortholog to the *act2* genes of *P. infestans*, *P. brassicae*, *P. melonis* and *Pythium splendens* (100% identity). *act2* present higher identity to the ascomycetous genes 91%, rather than 78% of *act1*.

*tub1* show 100% identity to *P. infestans* and *P. sojae* and 70% to *Y. lipolytica*, *K. lactis* and *S. cerevisiae*.

### 3D Structure of Actin1, Actin2 and Tubulin1

After obtaining the deduced amino acid sequence of the *act1*, *act2* and *tub1* genes we have determined the 3D structure of the proteins using the InterProScan program.

*act1* (Figure 2A) presents 82.3% of identity with the 3D structure of the reference protein 3ci5A and *act2* (Figure 2B) presents 86.9% of identity with the 3D structure of the reference protein 3eksA (described in the data bases). *tub1* encodes for a  $\alpha$ -tubulin protein and presents

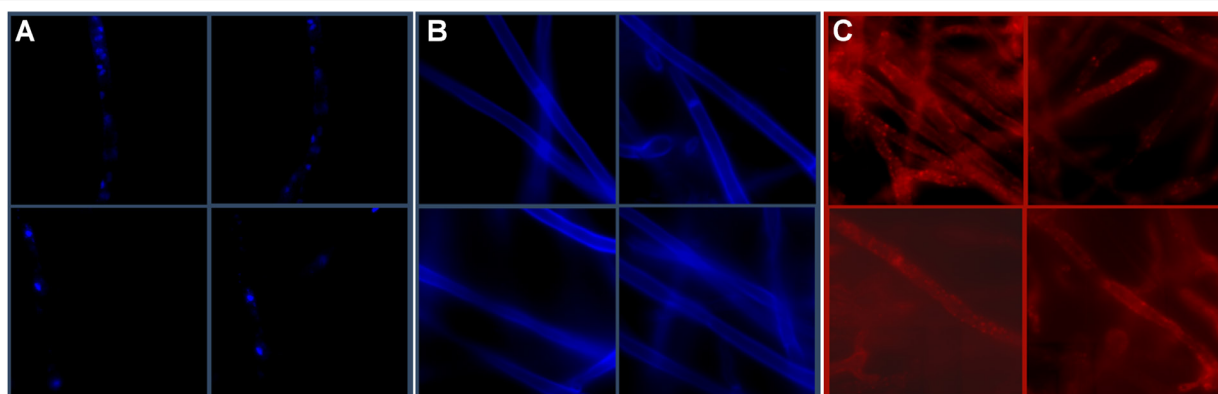


**Figure 1:** Fluorescence microscopy of stained *P. cinnamomi* mycelium at different locations. **A)** Each mycelium presents more than one individualized nucleus when stained with DAPI (1 mg/ml); **B)** A lack of division septa and actin cytoskeleton is observed in a cell wall stained with Calcofluor white (50 mg/ml); **C)** Actin distribution appears more concentrated at the hyphae extremities and adjacent to the plasma membrane when actin cytoskeleton was stained with Rhodamin-Phalloidin (0.1 µg/ml).

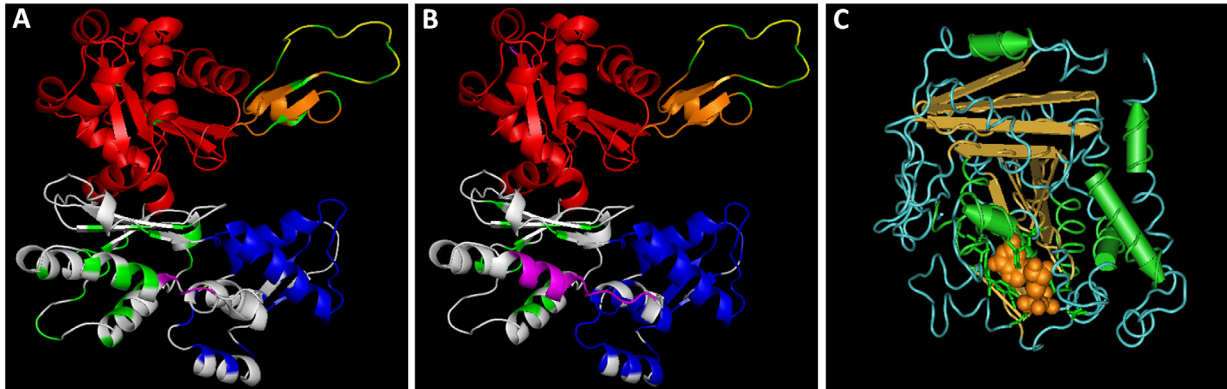


**Figure 2: 3D structures of Actin1, Actin2 and Tubulin1.** A) 3D structure of the protein encoded by *act1*, subdomain-1 is represented in red, subdomain-2 in orange, subdomain-3 in white subdomain-4 in blue; B) 3D structure of the protein encoded by *act2*, subdomain-1 is represented in red, subdomain-2 in orange, subdomain-3 in white subdomain-4 in blue. At subdomain-2 is represented the DNase I chain in yellow (as a loop); C) 3D structure of the protein  $\alpha$ -tubulin encoded by the gene *tub1*, in yellow we can observe the GTP subdomain.

76.3% of identity with the 3D structure of the reference protein 1Z2B of the data base. The high identity percentage with the reference protein sequences on the database, allowed us to determine the 3D structure of the proteins encoded by *tub1* (Figure 2C).

Looking at the 3D structure we can observe the actin proteins subdomains, represented in different colors (Figures 2A and B). Subdomain-1 is represented in red, subdomain-2 in orange, subdomain-3 in white subdomain-4 in blue. At the subdomain-2 is represented the DNase I chain in yellow (as a loop). Actin from many sources forms a tight complex with deoxyribonuclease (DNase I). The formation of this complex results in the inhibition of DNase I activity, and actin loses its ability to polymerize [18]. Also, subdomain-2 plays an important role in the movement of actin filaments *in vivo* [19]. In vertebrates, the four  $\alpha$ -actin isoforms present in various muscle cells and the  $\beta$ - and  $\gamma$ -actin isoforms present in no muscle cells differ at only four or five positions. Although these differences among isoforms seem minor, the isoforms have different functions:  $\alpha$ -actin is associated with contractile structures, and  $\beta$ -actin is at the front of the cell where actin filaments polymerize [20]. Actin exists as a monomer in low salt concentrations, but filaments form rapidly as salt concentration rises, with the consequent hydrolysis of ATP. Each actin protomer binds one molecule of ATP and has one high affinity site for either calcium or magnesium ions, as well as several low affinity sites. It has been shown that an ATPase domain of actin shares similarity with ATPase domains of hexokinase and hsp70 proteins.

Regarding the 3D structure of the observe the  $\alpha$ -tubulin protein, we can observe the  $\alpha$ -tubulin protein encoded by the gene *tub1* as well as the GTP domain (aa residues D82, T129, V161, S162, E167, N190, Y208). At microtubules the  $\alpha$ -tubulin subunit contains GTP while the  $\beta$ -tubulin subunit contains ATP. Microtubules assemble by polymerization of  $\alpha$ - $\beta$  dimers of tubulin. Polymerization is a polar process that reflects the polarity of the tubulin dimer, which in turn dictates the polarity of the microtubule [21]. To form microtubules, the dimers of  $\alpha$ - and  $\beta$ -tubulin bind to GTP and assemble onto the (+) ends of microtubules [5]. The energy to drive the microtubule machine comes from GTP hydrolysis. Tubulin is a GTPase whose activity is stimulated by polymerization. A crucial observation is that tubulin polymerizes in the presence of non-hydrolysable GTP to form stable microtubules. Thus, polymerization is driven by the high affinity of the tubulin-GTP dimer for the end of the microtubule [22].

Because of the extremely high diversity and adaptability of the oomycetes lifestyle it is imperative to dissect the multiple roles of the cytoskeleton and its functional interplay in a range of as many as possible species. Over the next few years more and more structural and regulatory components of the oomycete cytoskeleton will be localized and their dynamic interactions that ultimately generate function and determine cell form will be studied *in vivo*.

#### Acknowledgments

This study was supported by the project COMBATINTA/SP2.P11/02 Interreg IIIA-Cross-Border Cooperation Spain-Portugal, financed by The European Regional Development Fund.

#### References

1. Erwin DC, Ribeiro OK (1996) *Phytophthora* diseases worldwide, American Phytopathological Society Press, St. Paul, Minnesota, USA.
2. Abreu CG (1996) Doença da tinta: causas e consequências do declínio do castanhal. Estudos Transmontanos 6: 269-289.
3. Hardham AR (2005) *Phytophthora cinnamomi*. Mol Plant Pathol 6: 589-604.
4. Dominguez R, Holmes KC (2011) Actin Structure And Function. Annu Rev Biophys 40: 169-186.
5. Heald R, Nogales E (2002) Microtubule dynamics. J Cell Sci 115: 3-4.
6. Kabsch W, Holmes KC (1995) The actin fold. Faseb J 9: 167-174.
7. Walker SK, Chitcholtan K, Yu Y, Christenhusz GM, Garrill A (2006) Invasive hyphal growth: an F-actin depleted zone is associated with invasive hyphae of the oomycetes *Achlya bisexualis* and *Phytophthora cinnamomi*. Fungal Genet Biol 43: 357-365.
8. Ng R, Abelson J (1980) Isolation and sequence of the gene for actin in *Saccharomyces cerevisiae*. Proc Natl Acad Sci U S A 77: 3912-3916.
9. Unkles SE, Moon RP, Hawkins AR, Duncan JM, Kinghorn JR (1991) Actin in the oomycetous fungus *Phytophthora infestans* is the product of several genes. Gene 100: 105-112.
10. Raeder U, Broda P (1985) Rapid preparation of DNA from filamentous fungi. Letters in Applied Microbiology 1: 17-20.
11. Specht CA, DiRusso CC, Novotny CP, Ullrich RC (1982) A method for extracting high-molecular-weight deoxyribonucleic acid from fungi. Anal Biochem 119: 158-163.
12. Alfa C, Fantes P, Hyams J, McLeod M, Warbrick E (1993) Experiments with fission yeast: a laboratory course manual. Cold Spring Harbor Laboratory Press, Cold Spring Harbor, New York, USA.
13. Hanahan D (1983) Studies on transformation of *Escherichia coli* with plasmids. J Mol Biol 166: 557-580.

14. Michiels A, Tucker M, Van Den Ende W, Van Laere A (2003) Chromosomal walking of flanking regions from short known sequences in GC-rich plant genomic DNA. Plant Molecular Biology Reporter 21: 295-302.
15. Arnold K, Bordoli L, Kopp J, Schwede T (2006) The SWISS-MODEL workspace: a web-based environment for protein structure homology modelling. Bioinformatics 22: 195-201.
16. Guex N, Peitsch MC (1997) SWISS-MODEL and the Swiss-PdbViewer: an environment for comparative protein modeling. Electrophoresis 18: 2714-2723.
17. Schwede T, Kopp J, Guex N, Peitsch MC (2003) SWISS-MODEL: An automated protein homology-modeling server. Nucleic Acids Res 31: 3381-3385.
18. Lazarides E, Lindberg U (1974) Actin is the naturally occurring inhibitor of deoxyribonuclease I. Proc Natl Acad Sci U S A 71: 4742-4746.
19. Schwyter DH, Kron SJ, Toyoshima YY, Spudich JA, Reisler E (1990) Subtilisin cleavage of actin inhibits *in vitro* sliding movement of actin filaments over myosin. J Cell Biol 111: 465-470.
20. Lodish H, Berk A, Zipursky L, Matsudaira P, Baltimore D, et al. (2000) Molecular Cell Biology. (4th edn), WH Freeman and Company, New York, USA.
21. Howard J, Hyman AA (2003) Dynamics and mechanics of the microtubule plus end. Nature 422: 753-758.
22. Howard J, Hyman AA (2009) Growth, fluctuation and switching at microtubule plus ends. Nat Rev Mol Cell Biol 10: 569-574.